PHYSICAL REVIEW B VOLUME 45, NUMBER 11 15 MARCH 1992-I

Copper valence fluctuation in the organic conductor (dimethyl-N,N'-dicyanoquinonediimine)$_2$Cu studied by x-ray photoemission spectroscopy

I. H. Inoue and A. Kakizaki
Synchrotron Radiation Laboratory, Institute for Solid State Physics, University of Tokyo, Tanashi, Tokyo 188, Japan

H. Namatame and A. Fujimori
Department of Physics, University of Tokyo, Bunkyo-ku, Tokyo 113, Japan

A. Kobayashi
Department of Chemistry, University of Tokyo, Bunkyo-ku, Tokyo 113, Japan

R. Kato
Institute for Solid State Physics, University of Tokyo, Roppongi Minato-ku, Tokyo 106, Japan

H. Kobayashi
Department of Chemistry, Toho University, Funabashi, Chiba 274, Japan

(Received 16 July 1991)

We have studied the electronic structure of the organic conductor (DMe-DCNQI)$_2$Cu, where DMe-DCNQI is dimethyl-N,N'-dicyanoquinonediimine, by x-ray photoemission spectroscopy in order to elucidate the origin of the metal-insulator transitions and the anomalous magnetic properties of (DCNQI)$_2$Cu salts. The line-shape analysis of the Cu $2p$ core-level spectrum shows a Cu$^+$-Cu^{2+} mixed valency; the ratio of Cu$^+$ to Cu^{2+} is found to be nearly 2:1. This suggests that Cu is in a valence-fluctuating state in the metallic (DMe-DCNQI)$_2$Cu and that a Cu$^+$-Cu^{2+} charge ordering coupled with cooperative lattice distortion takes place below the metal-insulator transition temperature in other (DCNQI)$_2$Cu salts.

I. INTRODUCTION

A series of the most conductive organic salts that have ever been found, (R_1,R_2-DCNQI)$_2M$(R_1,R_2=CH$_3$, CH$_3$O,Cl,Br,I; DCNQI is N,N'-dicyanoquinonediimine; M=Cu, Ag, alkaline metals, NH$_4$, Tl) (Refs. 1 and 2), have attracted interest of many researchers. R_1,R_2-DCNQI are organic π-acceptor molecules which are uniformly stacked along the crystallographic c axis in one-dimensional columns. For the Cu, Ag, and Li salts, the cation is coordinated by four DCNQI molecules (Fig. 1), and, for the other salts, by six or eight DCNQI molecules.[2,3] The lowest unoccupied molecular orbitals of R_1,R_2-DCNQI, which consist of p_π orbitals, overlap to form a wide one-dimensional conduction band and are partially filled with electrons donated by the cations. This leads to the high conductivity along the stacking axis,[1,4] but they show metal-insulator (M-I) transitions at low temperatures. In the Ag salts, NH$_4$ salts, and the salts of the alkaline-earth metals, a fourfold $2k_f$ periodical distortion takes place through the formation of a charge-density wave (CDW) below $T_{M\text{-}I}\sim 100$ K,[5-7] which is attributed to the fact that the conduction band is quarter-filled due to the $1+$ oxidation state of these cations.

In the Cu salts such as (Me,Br-DCNQI)$_2$Cu, (DBr-DCNQI)$_2$Cu, and (Me,Cl-DCNQI)$_2$Cu [Me is CH$_3$ (methyl), DBr is Br,Br], on the other hand, the periodical distortion is threefold,[6,8] with a cooperative distortion of the coordination structures[2,8-10] of Cu at $T_{M\text{-}I}\sim 150$–230 K. This has been explained as due to the mixed valency of the Cu atoms, namely [Cu$^+$]:[Cu^{2+}]=2:1, leading to a $\frac{1}{3}$-filled conduction band. Some of the Cu salts [e.g., (DMe-DCNQI)$_2$Cu, (DMeO-DCNQI)$_2$Cu, and (Me,I-DCNQI)$_2$Cu; MeO is CH$_3$O (methoxy), DMe is CH$_3$,CH$_3$ (dimethyl), DMeO is CH$_3$O,CH$_3$O (dimethoxy)] do not show a M-I transition down to $T\sim 0.5$ K contrary to the other Cu salts. Under high pressure, however, the metal-

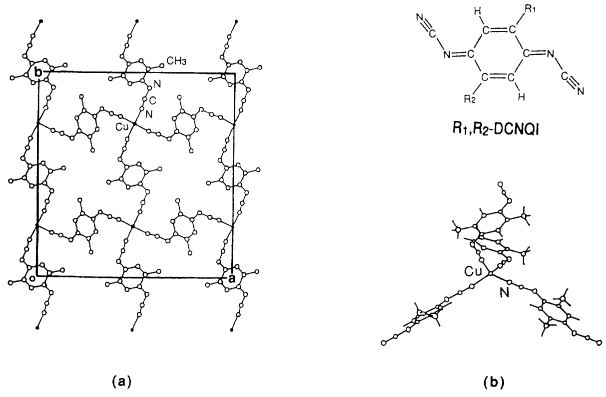

FIG. 1. (a) Crystal structure of (DMe-DCNQI)$_2$Cu. (b) R_1,R_2-DCNQI molecule and the coordination structure around Cu.

lic states become unstable,[11] showing M-I transitions of a reentrant type.[12,13] It has been proposed that these DCNQI-Cu systems behave like dense Kondo systems around the critical pressure above which the metallic state becomes unstable.[13] So far, electrical conductivities,[9,14,15] magnetic properties[8,9,14–17] pressure-phase diagram[18–20] as well as thermoelectric-power,[14] polarized-reflectance,[21] specific-heat,[16] and Fermi-surface calculations[22] have been reported.

If the Cu atoms are in a mixed-valent state, the x-ray photoemission spectroscopy (XPS) spectra of the Cu $2p$ core level of these salts should show satellite structures characteristic of the Cu^{2+} state.[23] Kobayashi *et al.*[8] reported the Cu $2p$ XPS spectra of $(DMe\text{-}DCNQI)_2Cu$ and $(Me,Br\text{-}DCNQI)_2Cu$ with marked satellite structures and estimated the Cu^{+}-to-Cu^{2+} ratio to be 2:1. On the other hand, Schmeissber *et al.* obtained spectra without such noticeable satellites and concluded that the satellite structures in the spectra of Kobayashi *et al.* are ascribed to Cu^{2+} species in surface contaminations and the oxidation state of Cu in the bulk DCNQI salts is close to 1+.[24] The purpose of the present work is therefore to clarify this point by careful examinations of the Cu $2p$ spectra in order to elucidate the nature of the M-I transitions in these compounds. We report the XPS spectra of $(DMe\text{-}DCNQI)_2Cu$ and their line-shape analyses, followed by a discussion about the electronic state of this and other Cu salts.

II. EXPERIMENT

Photoemission measurements were performed using a spectrometer having a base pressure of $\sim 10^{-10}$ Torr equipped with a Mg x-ray source for XPS and an electron gun for electron-energy-loss spectroscopy (EELS). Photoelectrons were collected with a double-pass cylindrical mirror analyzer (DCMA). The $(DMe\text{-}DCNQI)_2Cu$ samples we studied were black, thin needle crystals prepared by the diffusion method [reaction with CuI in acetonitrile (CH_3CN)]. We glued these needles side by side like a raft on an Al sample holder with conducting epoxy that could be solidified at room temperature. The samples were introduced into the spectrometer via an airlock and then mounted on a liquid-nitrogen cryostat. In order to obtain fresh, clean surfaces, we removed the surface layers by gently scraping with a diamond file in the ultrahigh-vacuum chamber because the surfaces of as-received samples were always contaminated by oxidation, etc. Since the core-level photoemission spectra of $(DMe\text{-}DCHQI)_2Cu$ are accompanied by plasmon satellites, we also measured EELS spectra in order to determine the energy and line shape of the plasmon peak. All the spectra reported here were measured at liquid-nitrogen temperature (~ 80 K) so as to prevent possible surface degradations, although, without our experimental accuracy, we found no difference between the spectra measured at liquid-nitrogen temperature and those measured at room temperature.

III. RESULTS AND DISCUSSION

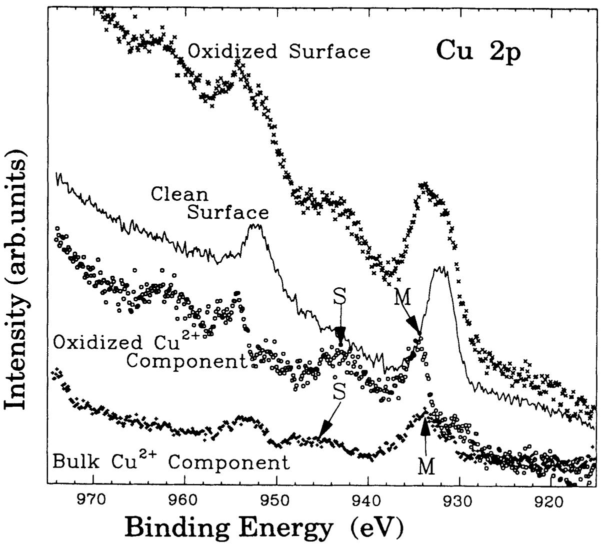

FIG. 2. Cu $2p$ core-level spectra of $(DMe\text{-}DCNQI)_2Cu$ without scraping (top), after scraping (next), and their difference (second from the bottom). The binding energies of the main (M) and satellite (S) peaks of the difference spectrum are equal to those of CuO, representing the oxidized surface contamination. The bottom is the spectrum of the bulk Cu^{2+} component that was extracted from the line-shape analysis (see Fig. 3). Note that the bulk Cu^{2+} spectrum is obviously different from that of the oxidized component.

As shown in Fig. 2, as-received samples with oxidized surfaces show pronounced satellite structures at ~ 945 eV as reported by Kobayashi *et al.*[8]; in the present study these satellites could be removed by scraping the surfaces. The spectrum for the scraped surface is highly reproducible, and its Cu^{2+} component (obtained by the decomposition of the spectrum into Cu^{2+} and Cu^{+} components as described below) is different in position and shape from that of the oxidized Cu^{2+} species on the surfaces (Fig. 2). This indicates that the Cu^{2+} signals observed for the scraped surfaces are not ascribed to surface contamination, but rather to Cu^{2+} in bulk $(DMe\text{-}DCNQI)_2Cu$. The presence of Cu^{2+} in bulk samples has also been supported by ESR measurements.[14–16]

In Fig. 3 (top) the spectrum of the scraped surface is shown with an appropriate correction for the transmission characteristics of the DCMA. The line shape of the spectrum resembles that reported by Schmeisser *et al.*[24] At first glance, it appears that the spectrum simply consists of a $2p_{1/2}$-$2p_{3/2}$ spin-orbit doublet and only Cu^{+} exists. However, there is a weak feature at ~ 945 eV, which may be attributed to the satellite of Cu^{2+}. Furthermore, the shape of the main peak at ~ 932 eV is evidently asymmetric with a significant tail on the high-binding-energy side; this asymmetry is not seen in the Cu^{+} spectra[23] and can be assigned to an overlapping Cu^{2+} feature. Therefore, we have decomposed the Cu $2p$ spectrum into Cu^{+} and Cu^{2+} components by a least-squares line-shape analysis method. In the line-shape analysis, each peak was assumed to be Lorentzian with the natural widths of the Cu $2p$ core level plus the Mg $K\alpha$ source[25] convoluted with a Gaussian. The Gaussian widths for the Cu^{2+}

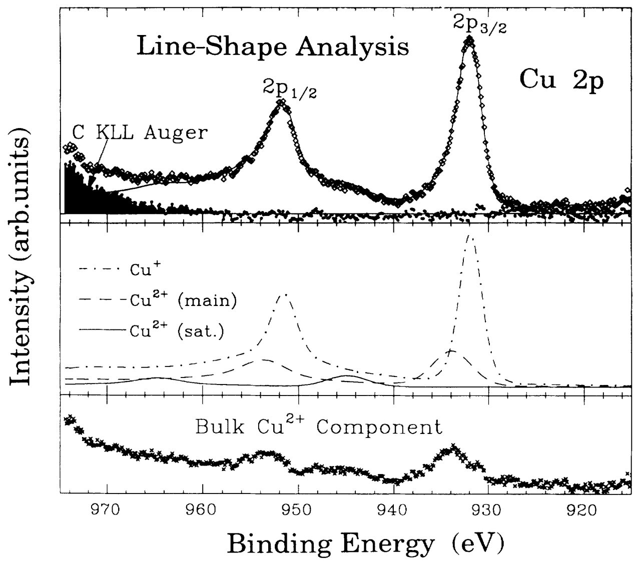

FIG. 3. Line-shape analysis of the Cu $2p$ XPS spectrum of (DMe-DCNQI)$_2$Cu. The spectrum is fitted by a superposition of Cu$^+$ and Cu^{2+} spectra. The Cu^{2+} component is further decomposed into the main and satellite peaks. Since the satellite of the Cu^{2+} component reflects the multiplet structures and its precise line shape is not known, we also show the spectrum obtained by subtracting the Cu$^+$ component from the raw data (bottom).

peaks are larger than that of Cu$^+$, because the ligand bandwidth and multiplet splitting contribute to the main peak and satellite of Cu^{2+}, respectively (Fig. 3 and Table I). In order to estimate the [Cu$^+$]:[Cu^{2+}] ratio with sufficient accuracy, it was necessary to take into account the overlapping plasmon-loss satellites accompanying the photoemission peaks because these satellites may affect the results of the line-shape analysis considerably. The energy and width of the plasmon peak have been obtained from the EELS spectrum as shown in Fig. 4 and Table I. The most prominent effect of the plasmon satellite accompanying the Cu $2p_{3/2}$ main peak is the broad feature centered at ~953 eV overlapping the Cu $2p_{1/2}$ peak. It should be noted that the feature at ~945 eV, which we have assigned to the Cu^{2+} satellite, can never be explained by the plasmon satellite. Thus we have decomposed the Cu $2p$ spectrum as shown in Fig. 3 (middle) and Table I, and concluded that the [Cu$^+$]:[Cu^{2+}] ratio is 2:(0.9±0.1). The binding-energy shift between the main peaks of Cu^{2+} and Cu$^+$ is found to be ~2 eV, as compared to ~1 eV between Cu$_2$O and CuO.[23] This large peak separation in (DMe-CDNQI)$_2$Cu may reflect the large stabilization energy of the Cu^{2+} state in the ground state due to the strong Cu $3d$–ligand hybridization as described below.

According to Schmeisser *et al.*, the shape of the Cu $2p$ XPS spectrum of (Me,Cl-DCNQI)$_2$Cu, which shows a M-I transition at 210 K, is very similar to that of (DMe-DCNQI)$_2$Cu; moreover, its line shape does not change across $T_{M\text{-}I}$. This result combined with our results leads us to speculate that the M-I transition occurs without a significant change in the valence mixing ratio and therefore that, in the charge-ordered insulating phase, the [Cu$^+$]:[Cu^{2+}] ratio should be almost exactly 2:1.

Now we will derive parameters that characterize the local electronic structure of the Cu^{2+} ion coordinated by N atoms, i.e., the CuN$_4$ cluster, from the analysis of the Cu $2p$ spectrum following the procedure of van der Laan *et al.*[26] The parameters are the energy difference, Δ, between the $3d^9$ and $3d^{10}\underline{L}$ states ($\underline{L}$ stands for a hole in the ligand N $2p$ molecular orbital that has the same symmetry as the d hole),

$$\Delta \equiv E(3d^{10}\underline{L}) - E(3d^9) ,$$

and the transfer integral, T,

$$T \equiv \langle 3d^9|H|3d^{10}\underline{L}\rangle \quad (>0) .$$

TABLE I. Fitted parameters for the line shape of the Cu $2p$ core-level XPS spectrum of (DMe-DCNQI)$_2$Cu. The Lorentzian width (LW) consists of the natural width of the Cu $2p$ core level and that of the Mg $K\alpha_{1,2}$ source (Ref. 25). The natural width of the Cu $2p_{1/2}$ peaks is larger than that of Ref. 25 due to $L_2L_3M_{4,5}$ ($2p_{1/2}$-$2p_{3/2}$-$3d$) Coster-Kronig transitions. Instead of considering the multiplet structures for the Cu^{2+} satellite peak, the Gaussian width (GW) of the Cu^{2+} satellite is assumed to be larger than that of Cu$^+$. Also the width of the Cu^{2+} main peak is larger than that of Cu$^+$ due to the ligand-hole contribution of the $\underline{c}d^{10}\underline{L}$ final state. The Gaussian width of the plasmon is assumed to be the same as that of the corresponding main peak. (FWHM denotes full width at half maximum.)

	Binding energy (eV)	Spin-orbit splitting (eV)	$2p_{3/2}$ LW (FWHM) (eV)	$2p_{1/2}$ LW (FWHM) (eV)	GW FWHM (eV)
Cu$^+$	931.8	19.66	0.92	1.47	1.92
Cu^{2+} (main)	933.8	19.76	0.92	1.47	3.63
Cu^{2+} (satellite)	945.0	19.76			4.10

	Energy (eV)	Extra LW (FWHM) (eV)
Plasmon	21.4	3.2

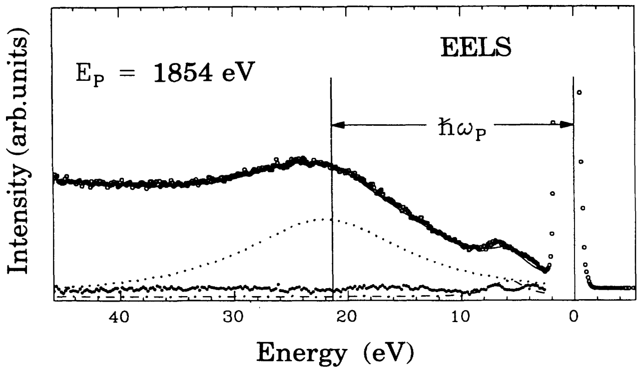

FIG. 4. EELS spectrum of $(\text{DMe-DCNQI})_2\text{Cu}$ taken with a primary electron energy of ~1850 eV and its line-shape analysis. Plasmon energy thus estimated (21.4 eV) coincides with the value calculated from the density of the total valence electrons (21.42 eV).

Then the ground state of the Cu^{2+} state is a bonding state between the d^9 and $d^{10}\underline{L}$ states as shown in Fig. 5 and is given by

$$\Psi_g(\text{Cu}^{2+})=\cos\theta|3d^9\rangle-\sin\theta|3d^{10}\underline{L}\rangle ,$$

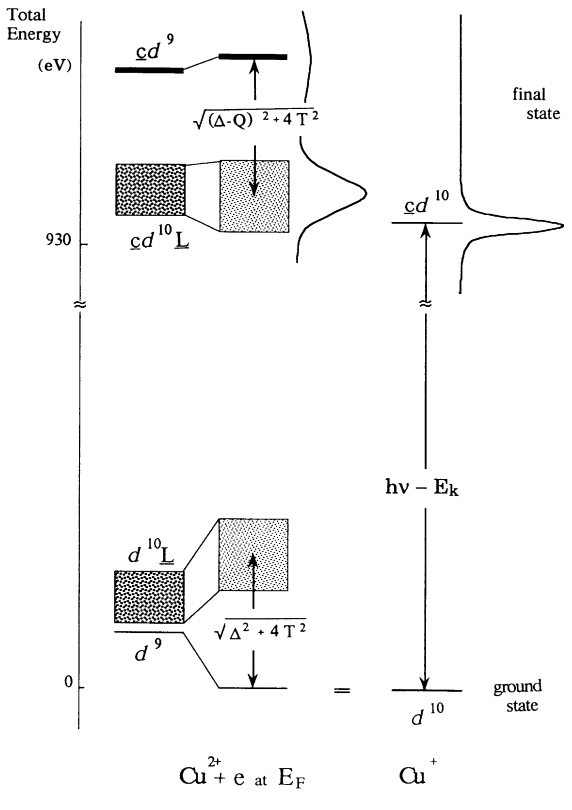

FIG. 5. Schematic energy-level diagrams in the ground state and final state for the Cu $2p$ core-level XPS of $(\text{DMe-DCNQI})_2\text{Cu}$. In the ground state, the valence fluctuation occurs between $\Psi_g(\text{Cu}^+)=|3d^{10}\rangle$ and $\Psi_g(\text{Cu}^{2+})=\cos\theta|3d^9\rangle-\sin\theta|3d^{10}\underline{L}_\sigma\rangle$. The creation of a $2p$ core hole raises the $\underline{c}3d^9$ level relative to the $\underline{c}d^{10}\underline{L}$ level by the core hole–$3d$ hole Coulomb repulsion energy Q.

where

$$\tan 2\theta=2T/\Delta \quad (0<\theta<\pi/2) ,$$

and has an energy of

$$E_g=E_0+\frac{\Delta}{2}-\frac{(\Delta^2+4T^2)^{1/2}}{2} ,$$

where $E_0\equiv E(3d^9)$. The final states of the Cu $2p$ XPS have a core hole on the Cu site. The Coulomb repulsive energy between the d hole and the core hole, Q, raises the energy of the $3d^9$ state with respect to the $3d^{10}\underline{L}$ state (Fig. 5). With the multiplet splitting being neglected, the final-state energies are given by

$$E_{s,m}=E_0'+\frac{\Delta}{2}\pm\frac{(\Delta-Q)^2+4T^2]^{1/2}}{2} ,$$

where $E_0'\equiv E(\underline{c}3d^9)$ and the subscripts s and m denote the final states corresponding to the satellite,

$$\Psi_s(\text{Cu}^{2+})=\sin\theta'|\underline{c}3d^9\rangle+\cos\theta'|\underline{c}3d^{10}\underline{L}\rangle ,$$

and the main peak,

$$\Psi_m(\text{Cu}^{2+})=\cos\theta'|\underline{c}3d^9\rangle-\sin\theta'|\underline{c}3d^{10}\underline{L}\rangle .$$

Here, $\underline{c}$ stands for the core hole and

$$\tan 2\theta'=2T/(\Delta-Q) \quad (0\leq\theta'\leq\pi/2) .$$

The energy separation between the main peak and the satellite is given by

$$W=E_s-E_m=[(\Delta-Q)^2+4T^2]^{1/2} .$$

In the sudden approximation, the intensities of the satellite and main peaks are given by

$$I_i=|\langle\Psi_i(\text{Cu}^{2+})|\Psi_g(\text{Cu}^{2+})\rangle|^2 \quad (i=s,m) ,$$

and their ratio by

$$\frac{I_s}{I_m}=\tan(\theta'-\theta)^2 .$$

From the experimentally derived values of $I_s/I_m=0.3\pm0.05$ and $W=11.2\pm0.2$ eV, we can estimate values for T and Δ as shown in Fig. 6, where the Δ and Q of other Cu^{2+} compounds are also plotted. Since we have only two experimental values, I_s/I_m and W, for the three unknown parameters, T,Δ, and Q, these parameters cannot be uniquely determined without further assumption. Therefore, by assuming that the intra-atomic quantity Q does not change much with substances and taking it to be ~9.6 eV, we could obtain $\Delta=0.3\pm0.7$ eV and $T=3.0\pm0.7$ eV. This small Δ is consistent with the low electronegativity of the N atom compared to Br and F. Because of the small Δ and large T, the $3d^9$ state and $3d^{10}\underline{L}$ configurations are strongly hybridized in the ground state.

The large T value estimated above is attributed to the σ bonds between the Cu $3d$ orbitals and the ligand N $2p_\sigma$ orbitals of DCNQI. In this picture, the metallic state is regarded as a valence-fluctuating state between the Cu^+ state $[\Psi_g(\text{Cu}^+)=|3d^{10}\rangle]$ and the Cu^{2+} state

$[\Psi_g(\mathrm{Cu}^{2+})=\cos\theta|3d^9\rangle-\sin\theta|3d^{10}\underline{L}_\sigma\rangle]$ as shown in Fig. 5. The strong $p_\sigma-d$ (d^9-$d^{10}\underline{L}_\sigma$) hybridization lowers the $\Psi_g(\mathrm{Cu}^{2+})$ state, leading to the degeneracy of the $\Psi_g(\mathrm{Cu}^{2+})$ and $\Psi_g(\mathrm{Cu}^{+})$ states. Hence the valence fluctuation between them takes place.

In Fig. 7 we show the N 1*s* core-level spectrum. In (DMe-DCNQI)$_2$Cu, N is located at two different sites in equal numbers, and therefore the N 1*s* spectrum is expected to consist of two peaks with equal intensities. However, the spectrum has actually such an asymmetric line shape that we could not decompose it into two peaks with equal intensities; instead we could decompose it into three peaks as shown in Fig. 7. As the intensity ratio is approximately 3:2:1 (*a* :*b* :*c* in Fig. 7), we infer that one of the two sites is further differentiated into two states (*b* and *c*). We thus consider that peak *a* is from the site which is the constituent of the imine, peak *b* is from the site coordinating to Cu$^+$, and peak *c* is from the site coordinating to Cu^{2+}, which is again consistent with the [Cu$^+$]:[Cu^{2+}] ratio of ~2:1. The mean valence of Cu, ~1.3+, derived in the present study is in good agreement with that determined by the recent infrared-absorption study of the N=C stretching vibration in (MeBr-DCNQI)$_2$Cu.[27]

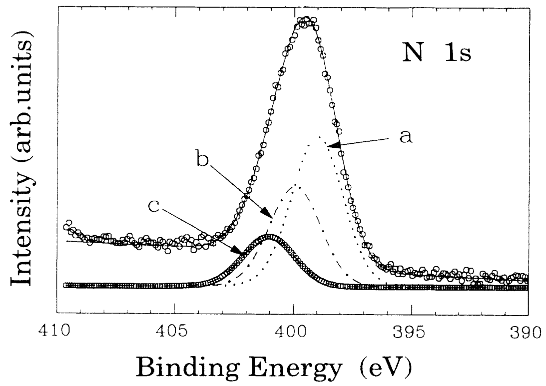

FIG. 7. N 1*s* core-level XPS spectrum of (DMe-DCNQI)$_2$Cu and its line-shape analysis. For details, see text.

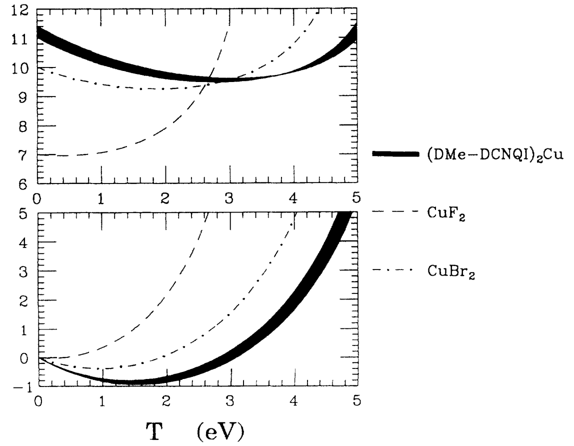

FIG. 6. Charge-transfer energy Δ and the core hole–3*d* hole Coulomb energy *Q* as functions of the ligand p_σ–Cu 3*d* transfer integral *T* for the observed values of E_s-E_m and I_s/I_m (see text). For comparison, dashed lines are those for CuF$_2$ and dashed-dotted lines are those for CuBr$_2$ taken from Ref. 26. The widths of the lines for (DMe-DCNQI)$_2$Cu correspond to the experimental uncertainties in the E_s-E_m and I_s/I_m values.

In (R_1,R_2-DCNQI)$_2$Cu, the Cu atoms are coordinated in a D_{2d} distorted tetrahedral geometry by the terminal N atoms of the R_1,R_2-DCNQI molecules.[2,8] Contrary to the salts of other cations, this crystal distortion around the Cu atoms is sensitive to the substituents (R_1,R_2).[2,10] This can be related to the intermediate valency of the Cu atoms as follows. When the size of the substituents is large, the CuN$_4$ cluster remains relatively undistorted. Then the cluster is close to the T_d symmetry and $\Psi_g(\mathrm{Cu}^+)$ is stabilized through bond formation between the ligand p_σ orbitals and the $4s4p^3$ hybrids of Cu. When the substituents are small, the CuN$_4$ cluster is distorted towards the square-planar configuration resulting in the increase of the p_σ-d covalency and the stabilization of $\Psi_g(\mathrm{Cu}^{2+})$.

Based on the above relationship between the distortion of the CuN$_4$ cluster and the relative stability of the Cu^{2+} and Cu$^+$ states, we can restate the observed dependence of $T_{M\text{-}I}$ on the substituents as follows: When $\Psi_g(\mathrm{Cu}^+)$ is relatively stabilized, the *M-I* transition does not occur and the system remains metallic. When the stability of $\Psi_g(\mathrm{Cu}^{2+})$ is increased, on the other hand the *M-I* transition takes place; the $T_{M\text{-}I}$ tends to rise with increasing stability of $\Psi_g(\mathrm{Cu}^{2+})$.[8] This can be understood as described below, if we assume that Cu in the metallic phase is in a valence-fluctuating state (i.e., in a "homogeneously-mixed-valent" state) through exchanging electrons with the p_π conduction band.

In the valence-fluctuating state, the position of the Fermi level in the p_π band is determined so that $\Psi_g(\mathrm{Cu}^+)$ and $\Psi_g(\mathrm{Cu}^{2+})$ (plus an electron at the Fermi level) are energetically degenerate. Therefore, since the position of the Fermi level depends on the number of conduction electrons supplied by the cations and hence on the mean valence of Cu, the mean valence of Cu in the metallic state is determined by the ionization level of $\Psi_g(\mathrm{Cu}^+)$ [or, equivalently, the affinity level of $\Psi_g(\mathrm{Cu}^{2+})$] relative to the p_π conduction band. If the Fermi level coincides with the latter level when the mean valence of Cu is 1.33+, the valence fluctuation occurs with the ratio [Cu$^+$]:[Cu^{2+}]=2:1 and it becomes possible that a Cu charge ordering occurs in a threefold unit-cell volume if the total energy of the system is lowered through, e.g., coupling between the charge ordering and the cooperative lattice distortion. Then the substituent dependence of $T_{M\text{-}I}$ can be naturally explained under the assumption that the [Cu$^+$]:[Cu^{2+}] ratio is slightly larger than 2:1 in (DCNQI)$_2$Cu salts with large substituents, and that charge ordering cannot occur because of the incommensurate [Cu$^+$]:[Cu^{2+}] ratio. Then, by changing the substituents from the larger to smaller ones, the Cu$^+$/Cu^{2+} ionization/affinity level can be lowered and the ratio approaches 2:1.

Thus we may conclude that the degeneracy of $\Psi_g(\mathrm{Cu}^+)$ and $\Psi_g(\mathrm{Cu}^{2+})$ occurring with the accidental commensuration of the $[\mathrm{Cu}^+]$:$[\mathrm{Cu}^{2+}]$ ratio drives the *M-I* transition in some $(\mathrm{DCNQI})_2\mathrm{Cu}$ salts. The effect of the pressure on the *M-I* transition can be explained within the same framework.[11,12] When we apply the pressure to the metallic $(\mathrm{DCNQI})_2\mathrm{Cu}$ salts to distort the CuN_4 cluster toward the square-planar configuration, $\Psi_g(\mathrm{Cu}^{2+})$ is stabilized and the system tends to show the *M-I* transition as stated above.[11,12]

In the above picture, $3d$ electrons in the $\mathrm{Cu}^+(d^{10})$ and $\mathrm{Cu}^{2+}(d^9\text{-}d^{10}\underline{L}_\sigma)$ states are assumed to be localized in the zeroth-order approximation and are not taken into account in the formation of Fermi surfaces satisfying Luttinger's sum rule.[28] Thus the one-dimensional conduction band is $\frac{1}{3}$ filled, leading to the instability of the metallic state accompanied by the threefold lattice distortion. So far, we have considered the p_π conduction band and N $2p_\sigma$ states separately, assuming that the hybridization between the Cu $3d$ orbitals and the p_π band is considerably weaker than the local p_σ-d hybridization. Nevertheless, it should be remembered that the p_π-d hybridization is necessary in inducing the Cu^+-Cu^{2+} valence fluctuation or Kondo-type interaction between the localized Cu d states and the p_π-derived conduction-band states. Such hybridization may lead to the formation of a correlated narrow d band at the Fermi level as in valence-fluctuating f-electron systems. Although the p_π conduction band itself is almost purely one dimensional, hybridization with the Cu $3d$ states introduces coupling between the one-dimensional columns,[10] particularly in the metallic state. This point will have to be taken into account when considering the electronic states near the Fermi level or the narrow d band in the $(\mathrm{DCNQI})_2\mathrm{Cu}$ systems. In order to study these problems, detailed valence-band photoemission studies provide further valuable information.

In conclusion, the valence of Cu is fluctuating between Cu^+ and Cu^{2+} in the metallic $(\mathrm{DMe\text{-}DCNQI})_2\mathrm{Cu}$. In the localized picture of the Cu $3d$ electrons, the $3d^9$ state lowered by the strong hybridization with $3d^{10}\underline{L}$ is degenerate with the $3d^{10}$ state, leading to the valence fluctuation in the metallic state. By controlling the $\mathrm{Cu}^+/\mathrm{Cu}^{2+}$ ionization/affinity level through changing the substituents, the commensuration $[\mathrm{Cu}^+]$:$[\mathrm{Cu}^{2+}]=2$:1 can be realized and charge ordering takes place. Transition from a valence-fluctuating state to a charge-ordered state is a natural consequence of the strong coupling between the electronic charge distribution and atomic displacement, although no clear evidence for such phenomena has been found in valence-fluctuating rare-earth compounds.

ACKNOWLEDGMENTS

We would like to thank Professor S. Kagoshima, Professor T. Takahashi, and Professor K. Yakushi for useful discussions. This work was supported by a Grant-in-Aid from the Ministry of Education, Science and Culture of Japan.

---

[1] A. Aumüller, P. Erk, G. Klebe, S. Hünig, J. U. von Schütz, and H.-P. Werner, Angew. Chem. Int. Ed. Engl. **25**, 740 (1986).

[2] R. Kato, H. Kobayashi, A. Kobayashi, T. Mori, and H. Inokuchi, Chem, Lett. **1987**, 1579.

[3] S. Hünig, H. Meixner, T. Metzenthin, U. Langohr, J. U. von Schütz, H.-C. Wolf, and E. Tillmanns, Adv. Mater. **2**, 361 (1990).

[4] W. Koch and Z. Naturforsch. Teil A **45**, 148 (1990).

[5] R. Moret, P. Erk, S. Hünig, and J. U. von Schütz, J. Phys. (Paris) **49**, 1925 (1988).

[6] R. Moret, Synth. Met. **27**, B301 (1988).

[7] J. U. von Schütz, M. Bair, H. J. Gross, U. Langohr, H.-P. Werner, H.-C. Wolf, D. Schmeisser, K. Graf, W. Göpel, P. Erk, H. Meixner, and S. Hünig, Synth. Met. **27**, B249 (1988).

[8] A. Kobayashi, R. Kato, H. Kobayashi, T. Mori, and H. Inokuchi, Solid State Commun. **64**, 45 (1987).

[9] A. Kobayashi, R. Kato, H. Kobayashi, T. Mori, and H. Inokuchi, Solid State Commun. **65**, 1351 (1988).

[10] R. Kato, H. Kobayashi, A. Kobayashi, T. Mori, and H. Inokuchi, J. Am. Chem. Soc. **111**, 5224 (1989).

[11] T. Mori, K. Imaeda, R. Kato, A. Kobayashi, H. Kobayashi, and H. Inokuchi, J. Phys. Soc. Jpn. **56**, 3429 (1987).

[12] S. Tomic, D. Jérôme, A. Aumüller, P. Erk, S. Hünig, and J. U. von Schütz, Europhys. Lett. **5**, 553 (1988).

[13] H. Kobayashi, A. Miyamoto, R. Kato, A. Kobayashi, Y. Nishio, K. Kajita, and W. Sasaki, Solid State Commun. **72**, 1 (1989).

[14] T. Mori, H. Inokuchi, A. Kobayashi, R. Kato, and H. Kobayashi, Phys. Rev. B **38**, 5913 (1988).

[15] H.-P. Werner, J. U. von Schütz, H. C. Wolf, R. Kremer, M. Gehrke, A. Aumüller, P. Erk, and S. Hünig, Solid State Commun. **65**, 809 (1988).

[16] T. Mori, S. Bandow, H. Inokuchi, A. Kobayashi, R. Kato, and H. Kobayashi, Solid State Commun. **67**, 565 (1988).

[17] H. Kobayashi, R. Kato, A. Kobayashi, Y. Nishio, K. Kajita, and W. Sasaki, J. Phys. Chem. Solids **51**, 533 (1990).

[18] S. Tomic, D. Jérôme, A. Aumüller, P. Erk, S. Hünig, and J. U. von Schütz, Synth. Met. **27**, B281 (1988).

[19] S. Tomic, D. Jérôme, A. Aumüller, P. Erk, S. Hünig, and J. U. von Schütz, J. Phys. C **21**, L203 (1988).

[20] R. T. Henriques, S. Tomic, W. Kang, D. Jérôme, F. Brisset, P. Batail, P. Erk, S. Hünig, and J. U. von Schütz, Synth. Met. **27**, B333 (1988).

[21] K. Yakushi, A. Ugawa, G. Ojima, T. Ida, H. Tajima, H. Kuroda, A. Kobayashi, R. Kato, and H. Kobayashi, Mol. Cryst. Liq. Cryst. **181**, 217 (1990).

[22] P. Schulmever, Philos. Mag. Lett. **62**, 195 (1990).

[23] J. Ghijsen, L. H. Tjeng, H. Eskes, G. A. Sawatzky, and R. L. Johnson, Phys. Rev. B **42**, 2268 (1990).

[24] D. Schmeisser, K. Graf, W. Göpel, J. U. von Schütz, P. Erk, and S. Hünig, Chem. Phys. Lett. **148**, 423 (1988).

[25] M. O. Klause and J. H. Oliver, J. Phys. Chem. Ref. Data **8**, 329 (1979).

[26] G. van der Laan, C. Westra, C. Haas, and G. A. Sawatzky, Phys. Rev. B **23**, 4369 (1981).

[27] H. Kobayashi, A. Miyamoto, H. Moriyama, R. Kato, and A. Kobayashi, Chem. Lett. **1991**, 863.

[28] J. M. Luttinger, Phys. Rev. **119**, 1153 (1960).

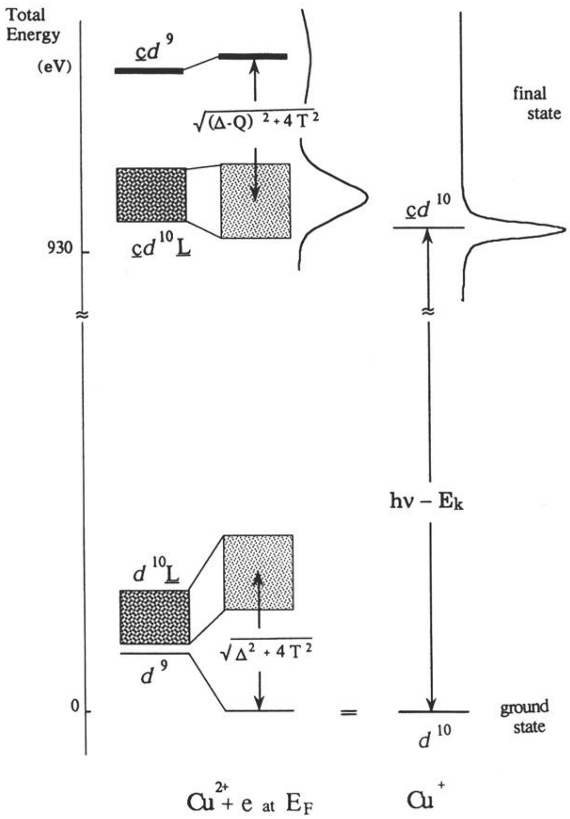

FIG. 5. Schematic energy-level diagrams in the ground state and final state for the Cu $2p$ core-level XPS of (DMe-DCNQI$)_2$Cu. In the ground state, the valence fluctuation occurs between $\Psi_g(\mathrm{Cu}^+)=|3d^{10}\rangle$ and $\Psi_g(\mathrm{Cu}^{2+})=\cos\theta|3d^9\rangle-\sin\theta|3d^{10}\underline{L}_\sigma\rangle$. The creation of a $2p$ core hole raises the $\underline{c}3d^9$ level relative to the $\underline{c}d^{10}\underline{L}$ level by the core hole–$3d$ hole Coulomb repulsion energy Q.